Magnonics: Spin Waves on the Nanoscale

By *Sebastian Neusser* and *Dirk Grundler**

Magnetic nanostructures have long been in the focus of intense research in the magnetic storage industry. For data storage the nonvolatility of magnetic states is of utmost relevance. As information technology generates the need for higher and higher data-transfer rates, research efforts have moved to understand magnetization dynamics. Here, spin waves and their particle-like analog, magnons, are increasingly attracting interest. High-quality nanopatterned magnetic media now offer new ways to transmit and process information without moving electrical charges. This new functionality is enabled by spin waves. They are confined by novel functioning principles, which render them especially suitable to operate at the nanoscale. Magnonic crystals are expected to provide full control of spin waves, similarly to what photonic crystals already do for light. Combined with nonvolatility, multifunctional metamaterials might be formed. We report recent advances in this rapidly increasing research field called magnonics.

1. Introduction

Spin dynamics phenomena in nanomagnets have generated large interest in recent years. In particular, the study of spin waves (SW) or magnons has attracted increasing attention. Magnons are the particle-like spin excitations in a magnetic material. The wave-like counterpart is referred to as SW. The advancements in deposition and nanopatterning techniques have now allowed the precise tailoring of these excitations in ferromagnetic materials. Thanks to these novel techniques, SW quantization,[1] localization,[2] and interference[3] have been observed for the first time. SWs exhibit both the classical and quantum-mechanical properties of waves. They can reflect when incident onto magnetic potential wells and can tunnel through magnetic barriers.[4,5]

Magnetic storage industry provides an important backbone of information technology. Data storage relies on non-volatility and long-term stability of magnetic states. This non-volatility has been used to ''program'' SW excitations of patterned magnets.[6,7] This means that nowadays, both, the static and dynamic properties of magnetic materials can be designed on the micro- and sub-micrometer scales. The recent achievements offer the perspective of magnetic-field-controlled devices in which SWs are used to carry and process information.[8] This newly born research field, namely magnonics, is growing exponentially.[9] Key magnonic components are currently explored, including magnonic wave guides, SW emitters, and filters.[10] Since the wavelength λ of magnons is orders of magnitude shorter than that of electromagnetic waves (photons) of the same frequency, magnonic devices are a powerful solution toward the fabrication of nanometer-scale microwave devices. Indeed, in magnetic wires, nano-optics with propagating SWs has been demonstrated.[11]

It is our opinion that periodically patterned magnetic media at the nanoscale will be used in the future. In these materials, the so-called minibands are formed. Minibands consist of allowed SW frequencies and forbidden frequency gaps, and are deterministically dependent on the pattern design.[12,13] Such magnonic crystals[12] can find their analogy in, for example, photonic crystals already explored in optical communication technology for the control and manipulation of light.[14] Especially challenging is the fact that the dispersion relations for SWs are far more complex than for photons. They are anisotropic in a homogeneous and isotropic material, as they depend on the relative orientation between the magnetization and the wave vector. An important consequence of this is that a confining potential (or confining well) applied in different spatial directions results in distinctly different SW modes.

At the same time, a patterned magnetic material generates static and dynamic stray fields. The demagnetization fields modify the dynamic response, in particular at the edges of the device.[15] As the devices shrink to the nanoscale, this influence of the edges becomes increasingly important. In this sense, many different device geometries have already been investigated, such as straight wires,[2,16] rectangles,[1] rings,[3] and disks.[17,18] In such nonellipsoidal devices, the demagnetization field is spatially inhomogeneous, and confines distinct SW modes at device boundaries: edge modes that drastically alter the dynamic properties are formed.[2,16] However, new interesting phenomena can also arise from non-collinear spins inside a magnet. For example, it has been recently found that the inhomogeneous magnetization of a nanowire results in the confinement of SWs *in the center* of the wire.[19] This effect opens bright perspectives for low-loss SW propagation in magnonic waveguides. Its action can be compared to refractive-index changes in optical fibers, which guide light waves remote from the fiber's edges. The reduced light scattering by graded-index fibers has pushed optical information technology enormously forward.

[*] Prof. D. Grundler, S. Neusser
Physik Department
Lehrstuhl für Physik funktionaler Schichtsysteme
Technische Universität München
James-Franck-Str. 1, D-85748 Garching (Germany)
E-mail: grundler@ph.tum.de

DOI: 10.1002/adma.200900809

© 2009 WILEY-VCH Verlag GmbH & Co. KGaA, Weinheim

Magnonic devices based on the phenomena described above have the potential to provide new functionalities with long-term interest beyond fundamental research. Several options are open for their future utilization. As an example, the long SW coherence length[20] could be used to process information in a coherent way. Before the scenario of applied magnonic devices becomes real, the understanding of spin excitations in topologically complex nanomagnets must be pushed forward and magnetic materials must be optimized.

In this paper, we first present basic characteristics of SWs in plain thin films, and follow with a discussion on recent observations in nanopatterned magnetic wires and antidot lattices. Finally, we conclude with some perspectives on future research opportunities.

2. Nanoscale Magnonic Devices

The important length scales for magnonic devices range from Angstroms to several hundred nanometers and micrometers depending on whether the SWs are dominated by short-ranged exchange interactions or by long-ranged dipolar interactions between spins. This wide range renders a theoretical treatment cumbersome. We present here a qualitative understanding for SWs in magnonic devices. Micromagnetic simulations help to illustrate the spin-precession amplitudes.[21]

The eigenfrequencies of SW excitations are determined by the spin stiffness (strength of exchange interaction), the absolute value of the saturation magnetization M_S, the wavevector $\vec{k}$, and, particularly interesting, the relative orientation between the magnetization vector $\vec{M}$ and the wavevector $\vec{k}$ with $k = 2\pi/\lambda$. In Figure 1a we display characteristic dispersion curves for a thin magnetic film in two limiting cases of in-plane magnetization.[21] Both, exchange interaction and dipolar forces, rule the characteristic slope of the SW dispersion relations and thereby the group velocity. When a thin film is excited locally by a magnetic-field pulse, SWs are found to propagate with anisotropic characteristics (Fig. 1b and c). The interplay between this anisotropic behavior and device boundaries in patterned magnets (as seen, for example, in Fig. 1d and e) is in one of the interesting foci of current research.[21] Experiments have been done on different materials such as ferrimagnetic yttrium iron garnets (YIG) and ferromagnetic metals such as Co, Fe, or permalloy ($Ni_{80}Fe_{20}$), which due to different spin stiffness and saturation magnetization address different SW frequency regimes, typically ranging from several 0.1 to few 10 GHz.

Furthermore, increasing (decreasing) the magnetic field in Figure 1a shifts the SW eigenfrequencies up (down). Importantly, the internal field H_{int} is relevant and includes the external field H, the demagnetization field H_{dm}, and further effective fields originating from material properties such as magnetocrystalline anisotropy, etc. As an example, we will discuss below magnonic devices that were fabricated from permalloy. In this example, it will be sufficient to consider $H_{int} = H + H_{dm}$.

Concluding, the dispersion curves in Figure 1a can be modified by the material, its film thickness, the external magnetic field, and, via H_{dm}, by the shape of the patterned magnet.

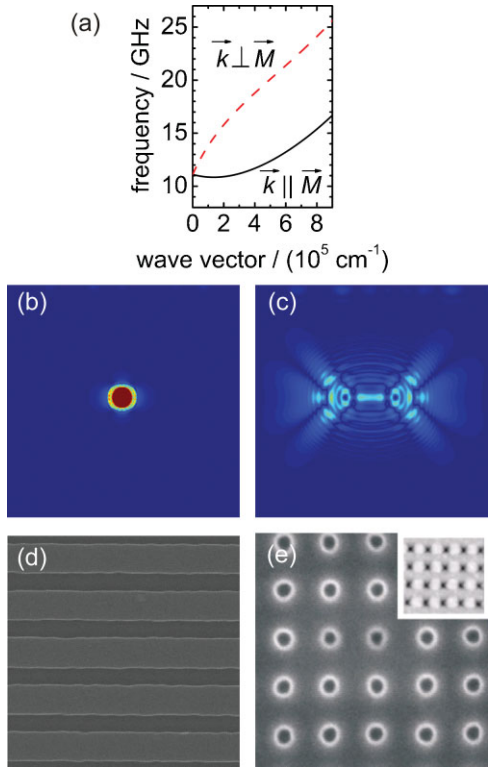

Figure 1. a) SW dispersion relations for different propagation directions. The permalloy film is assumed to be 16 nm thick in an applied in-plane field of $\mu_0 H = 130$ mT. b) Simulated excitation of the same film with a local-magnetic-field pulse forcing spins to misalign with the applied field (image taken about 1 ps after pulsed excitation (circle)). c) The spatial distribution of spin-precession amplitudes (bright color) after 250 ps reflects the complex magnon dispersion. For nanopatterned magnonic devices, the SW quantization conditions and propagation depend crucially on the orientation of M, inhomogeneities of H_{int}, and device design: d) 300-nm-wide wires fabricated by means of electron-beam lithography and lift-off processing of permalloy. Reproduced with permission [23]. Copyright 2009, American Institute of Physics. e) Antidot array in a permalloy film with unit-cell size of 490 nm. The holes (black) were fabricated by means of focused ion beam patterning. The inset shows, on the same scale, a permalloy-covered membrane from anodized alumina oxide providing nanopatterned holes (black, [35]b). Image courtesy of B. Botters, Technische Universität München.

2.1. From Magnetic Wires to a One-Dimensional Magnonic Crystal

Micrometer-wide wires have extensively been investigated by optical means, such as Brillouin light scattering (BLS)[2] and magneto-optical Kerr effect (MOKE),[16] as well as by all-electrical means.[22] Using spatially resolved techniques on permalloy wires with a width $\omega = 2000$ nm, center and edge SW modes were imaged. They were found to possess a large spin precession amplitude in the central (compare Fig. 2a) and the edge regions, respectively.[1,2,11,16] The mode localization depends on both the orientation of the magnetization M with respect to the edges of the wire and the exact SW eigenfrequency. Assume a SW of wave

WILEY InterScience DISCOVER SOMETHING GREAT

© 2009 WILEY-VCH Verlag GmbH & Co. KGaA, Weinheim

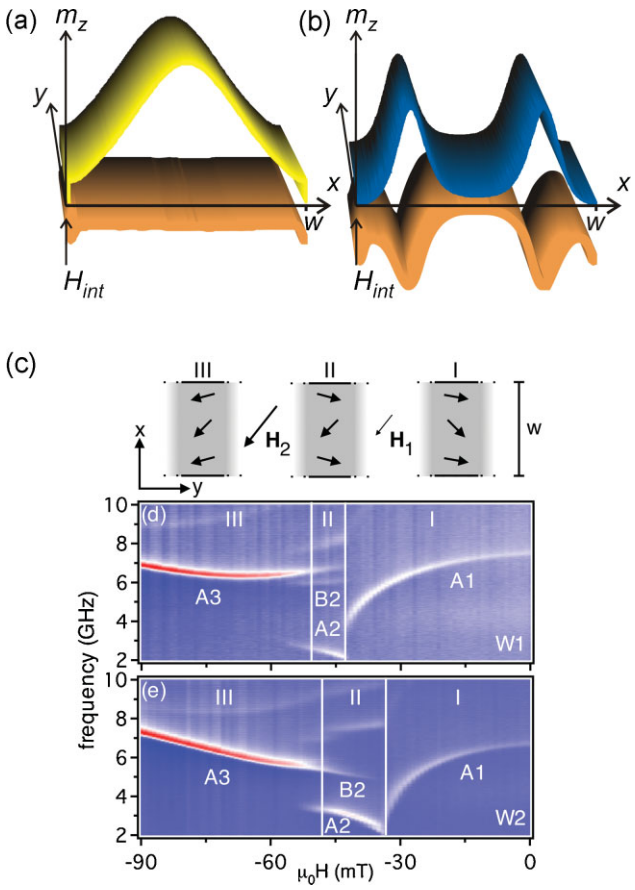

Figure 2. Spatial distribution of the precession amplitudes $m_z(x, y)$ in a permalloy wire for a) a center mode, where dipolar pinning at the edges is effective, and b) SW channeling induced by a zig-zag magnetization. c) Schematic spin configurations of a magnetic nanowire extending in the *y* direction in an in-plane magnetic field that is applied a few degrees off the *x* direction. The arrows indicate the local orientation of microscopic magnetic moments: in field regime II, only the moments in the central region of the wire have switched, and are aligned with *H*. The edge regions point nearly in the opposite direction. This leads to a zig-zag configuration of the magnetization *M*. Magnetic-field-dependent SW resonances measured on an array of 300 nm wide wires with an edge-to-edge separation of d) 700 nm and e) 200 nm. White and red colors reflect strong absorption of a microwave magnetic field. Reproduced with permission from [23]. Copyright 2009, American Institute of Physics. Modes A1 and A3 correspond to a center mode as displayed in a), mode A2 is shown in b).

vector $k^2=k_x^2+k_y^2$ in a wire extending along the *y* direction. In a longitudinally magnetized wire, the center mode is free to move along the wire but exhibits a specific wave vector in the *x* direction of $k_x=\pi/w'$. The parameter w' is the effective width of the wire, which is determined by dipolar pinning of individual magnetic moments at the edges. It is thus related to the physical width *w* of the wire.[15] Typically, w' is larger than *w*. Thereby, the SW center mode experiences a non-zero spin precession amplitude also at the device boundaries (compare Fig. 2a). In a transversely magnetized wire, an edge mode appears: the demagnetization field H_{dm} reduces the internal field H_{int} in particular at the edges of the wire. H_{int} becomes spatially inhomogeneous and the SW dispersions of Figure 1a vary as a function of distance from the edge of the wire; by this means, SW wells form and guide SWs along the edges of the wire.[2] If compared to light waves, the inhomogeneous H_{int} finds its analog in a gradually changing refractive index. For light, index variations have already been known for a long time, and have been functionalized to guide and confine the electromagnetic waves.[14]

In SW propagation experiments, the center modes were found to transmit SW information up to several micrometers along a wire in the *y* direction.[11] Recently, a novel mode was discovered that exhibited a width an order of magnitude smaller than the previously known center modes.[19,23] Here, scanning MOKE and BLS did not provide sufficient spatial resolution for imaging. Instead, the measurements were based on all-electrical broadband SW spectroscopy and interpreted via micromagnetic simulations.[19,21–23] The permalloy wires were 300 nm wide and arranged in a periodic array (Fig. 1d). In Figure 2d and e, magnetic-field-dependent spectra are displayed in a color-coded plot where bright color indicates SW eigenfrequencies. The edge-to-edge separation between nanowires is 700 and 200 nm, respectively.

The magnetic state of the wires was controlled via the magnetic history and applied magnetic field *H*. Initially, the wires were magnetized and saturated along the positive *y* direction, along the longitudinal axis of the wire. Then, the magnetic field was applied as indicated in the inset. The field now exhibited a component parallel to the negative *y* direction, energetically favoring reversal of the magnetization direction. The wires irreversibly reversed via a two-step process, that is, three characteristic field regimes I–III occurred (Fig. 2c–e). In regimes I and III, the center mode, as discussed above, was observed. The novel SW mode appeared in regime II, and was labeled A2. Micromagnetic simulations attribute this spin excitation to two 65 nm wide SW channels in parallel along the longitudinal axis of the wires (Fig. 2b). This small channel width originates from the underlying static domain configuration and not from the edges. In regime II, the wire's magnetization forms a zig-zag-shaped magnetic configuration, where spins only partially align with the external field *H* (Fig. 2c). This leads to uncompensated magnetic charges in the inner region of the wire, provoking two pronounced local minima of the internal field H_{int} (Fig. 2b). For the excited SW mode A2, the spin precession amplitude at the geometrical edges is small if compared to the center mode A1.[19] The new type of mode occurs irrespective of the exact edge-to-edge separation between the wires forming the array.[23]

The results suggest that SWs of type A2 might be compared to light waves guided in a graded-index optical fiber. In the latter case, a gradual change of the refractive index between the fiber's central and edge regions is achieved by different material compositions in the radial direction.[14] The tailored material composition leads to an internal confinement of the light wave, thereby reducing light scattering at the fiber's edges. The results of Figure 2 show that in a magnonic waveguide the internal field resulting from a zig-zag-shaped magnetic configuration provokes a similar effect for SWs. Due to the reduced amplitude at the edges, the SW should experience a reduced magnon scattering probability. Preliminary time-resolved experiments indeed showed that the relaxation time of mode A2 was about a factor of three larger than mode A1.

© 2009 WILEY-VCH Verlag GmbH & Co. KGaA, Weinheim

Densely-packed arrays of permalloy nanowires have recently been found to exhibit partial SW frequency gaps reminiscent of a one-dimensional magnonic crystal.[24] These wires were homogeneously magnetized and only 55 nm apart from each other. Though conceptually SWs are defined only inside a material, the periodic lattice of isolated magnetic wires can exhibit phase-coherent collective excitations via the long-range dipolar coupling. The translational symmetry of a densely packed array then gives rise to the observed miniband formation. A corresponding miniband effect has also been reported for micropatterned YIG waveguides, where the thickness was periodically modulated along the axis of the wire by etching grooves. Propagating SWs were reflected in a frequency band where the efficiency and frequency width depended on the groove depth.[25] These characteristics are technologically relevant for SW filters.

2.2. Antidot Lattices

Antidot lattices are periodic arrays of holes patterned into a thin film. Such lattice configurations are known from nanoelectronics[26] and photonics.[14] In case of magnetic devices, the expected functionality can be manifold: an antidot lattice can be i) a nonvolatile memory,[27] ii) a network of multiple connected magnonic wave guides,[28] iii) a 2D magnonic crystal,[29] and iv) the basis for a magnetic metamaterial.[30]

In the following, we explain SW eigenmodes in an antidot array in terms of a network of magnonic waveguides. Here, we representatively discuss a permalloy lattice with a period of 490 nm and hole diameter of 240 nm (Fig. 1e). The static domain configuration depends on the absolute field strength and orientation of the field.[27,28,31] For an in-plane field H larger than about 40 mT, the spins align with H and exhibit a preferential orientation throughout the lattice. In this field regime, pronounced SW resonances occur. A high degree of consistency is achieved between experimental data gained from all-electrical inductive microwave spectroscopy and data obtained from micromagnetic simulation (Fig. 3a–f). Fast-Fourier-transform imaging[18] of simulation data is used to illustrate spatial distributions of spin-precession amplitudes for different field orientations at $\mu_0 H = 100$ mT (Fig. 3g). Spin excitation at about 11 GHz leads to large precession amplitudes mainly between neighboring (top) or next-neighboring holes (bottom), depending on the orientation of the magnetic field. Interestingly, the mode patterns change completely for excitation at a smaller frequency around 8 GHz. The excitation now extends in wave guides between the holes through the lattice. It is found that their orientation is directly linked with the external magnetic field: the modes appear in a direction perpendicular to the field vector and magnetization direction. This is due to the demagnetization effect of the holes. Stray fields from the hole regions produce local extrema of H_{int}.[29] Here, spin excitation takes place. The modes thus reflect the periodic inhomogeneity of H_{int}. The precession amplitudes are surprisingly homogeneous in the direction perpendicular to H. If H is applied in a diagonal direction, the wave guides of large spin-precession amplitude are narrow, with a width of only 100 nm, much smaller than the lattice constant of 500 nm (Fig. 3g, bottom row on the right).

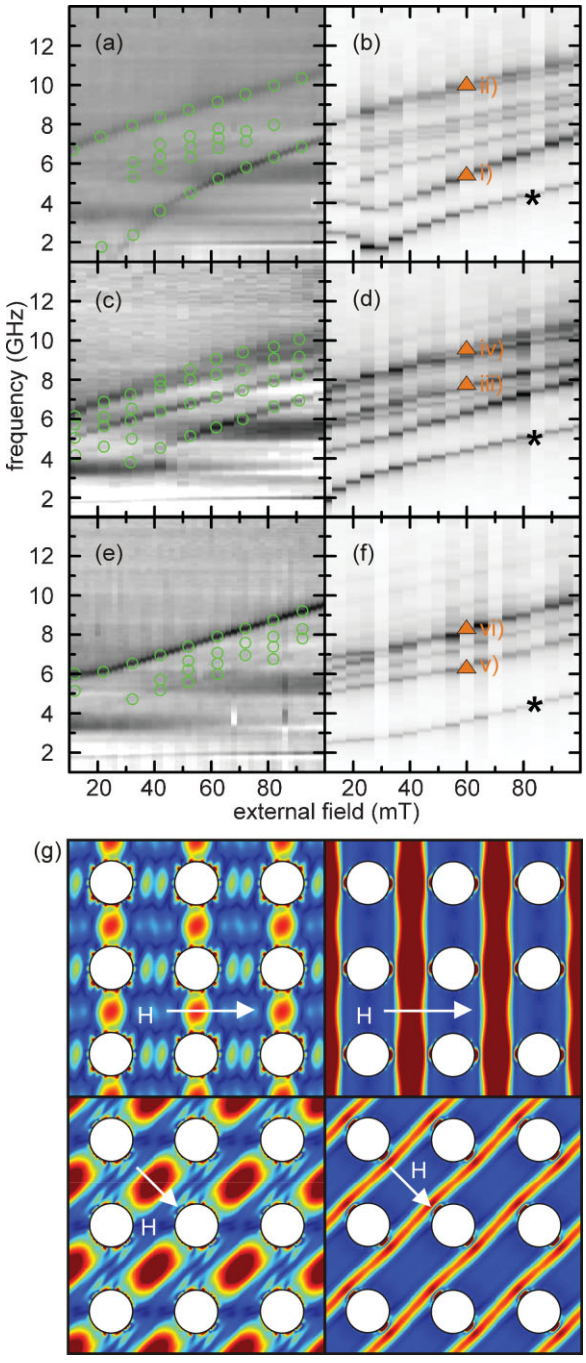

Figure 3. SW resonances in an antidot lattice for three different magnetic-field orientations: field applied under 0° (a, b), 25° (c, d), and 45° (e, f) with respect to a principal lattice axis. The lattice constant (hole diameter) is 490 (240) nm. Experimental data (left), where SW resonances are highlighted by open circles, are compared to simulation results (right). Dark represents strong absorption of a microwave magnetic field. The mode marked by the asterix is not resolved in the experiment, most likely due to unintentional edge roughness. Triangles mark the types of modes discussed in the text. Reproduced with permission from [31]. Copyright 2008, American Institute of Physics. g) Color-coded spin-precession profiles for an in-plane field of $\mu_0 H = 110$ mT applied under 0° in horizontal direction (top row) and 45° (bottom row). The left column reflects resonant excitation at high frequencies above 10 GHz. The right column is for about 8 GHz. Red color represents large precession amplitudes.

WILEY InterScience DISCOVER SOMETHING GREAT
© 2009 WILEY-VCH Verlag GmbH & Co. KGaA, Weinheim

In time-resolved simulations, one finds that SWs excited by a broadband magnetic-field pulse on one side of an antidot lattice propagate only when the magnetic field is perpendicular to the propagation direction.[28] When reaching the other side, selective wave vectors and frequencies appear. Such a filtering effect is known from photonics, where the translational symmetry of an antidot lattice modifies the dispersion relations and density of states.[14] For SWs, however, turning the field of 100 mT by 90° is found to block the transmission. This external control of propagation through a network of magnonic wave guides by moderate fields underscores the novel functionality of periodically patterned magnetic materials.

3. Conclusions

In the past few years, experiments have demonstrated the basic principles of how to tailor SWs in ferromagnetic materials. SW confinement on the 100 nm scale and below has been achieved by nanopatterning combined with internal field profiles of a well-defined magnetization configuration. In future experiments, such configurations might be stabilized in the remanent state. This will open a great avenue of technological applications. The stabilization could happen by specifically designed ion irradiation[32] or by adding an exchange-coupled antiferromagnetic underlayer exhibiting the appropriate domain configuration. By this means, a periodic magnetization configuration would generate the desired SW dynamics, as imprinted into the magnonic device. Wisely tuned SW confinement already allows for efficient SW transmission due to reduced scattering, providing a large signal-to-noise ratio in potential technical application. So far, however, we have focused on specific device designs. Further improvements on SW damping are offered by novel materials. Heusler alloys, where the half-metallicity suggests the absence of some elementary magnon scattering processes, might be particularly interesting.[33] Here, fundamental studies on SW damping are still at their infancy.[34]

For antidot lattices, optimized unit-cell configurations and deep-sub-micrometer lattice constants open up possibilities to generate prominent minibands and forbidden frequency gaps in two spatial directions. Short-period lattices will address SW modes that are dominated by exchange interaction rather than by dipolar interactions, as discussed here. Anodized alumina membranes with highly ordered arrays of holes might represent suitable short-period nanotemplates (compare inset in Fig. 1e).[35] Exchange-dominated SWs might increase the operational frequency range of SW filters to the several-10-GHz regime depending on the material. Several theoretical studies on magnonic crystals have already been presented.[13,36–38] Innovative materials research will be needed to generate two-component magnetic superstructures that promise complete band gaps in three dimensions.[13] Top-down fabrication processes, as discussed here, might then be overtaken by bottom-up approaches.[39–41] Intentionally introduced nanodefects should then be explored to provide storage devices for SW information. Advanced device concepts will address periodically patterned magnets as metamaterials, where the field-controlled and programmable dynamic response offers multifunctionality up to optical frequencies by the design of the nanostructures.[30]

Understanding the wave phenomena of both electrons and light created powerful electronic and photonic devices; based on artificially tailored solids, sophisticated means were engineered to control and manipulate such waves down to the nanoscale.[14] These achievements significantly promoted modern information technology. For SW control and manipulation, we are at the beginning, but recent results already promise intriguing possibilities. Despite numerous challenges in magnonics, further exciting advancements can be expected for the future.

Acknowledgements

The authors thank M. Becherer, B. Botters, F. Giesen, D. Heitmann, A. Holleitner, K. Nielsch, J. Podbielski, C. A. Ross, D. Schmitt-Landsiedel, and J. Topp for support. We acknowledge financial support by the Excellence Cluster ''Nanosystems Initiative Munich (NIM)''.

[1] C. Mathieu, J. Jorzick, A. Frank, S. O. Demokritov, A. N. Slavin, B. Hillebrands, B. Bartenlian, C. Chappert, D. Decanini, F. Rousseaux, E. Cambril, *Phys. Rev. Lett.* **1998**, *81*, 3968.
[2] J. Jorzick, S. O. Demokritov, B. Hillebrands, M. Bailleul, C. Fermon, K. Y. Guslienko, A. N. Slavin, D. V. Berkov, N. L. Gorn, *Phys. Rev. Lett.* **2002**, *88*, 047204.
[3] J. Podbielski, F. Giesen, D. Grundler, *Phys. Rev. Lett.* **2006**, *96*, 167207.
[4] T. Neumann, A. A. Serga, B. Hillebrands, M. P. Kostylev, *Appl. Phys. Lett.* **2009**, *94*, 042503.
[5] U.-H. Hansen, M. Gatzen, V. E. Demidov, S. O. Demokritov, *Phys. Rev. Lett.* **2007**, *99*, 127204.
[6] F. Giesen, J. Podbielski, T. Korn, M. Steiner, A. van Staa, D. Grundler, *Appl. Phys. Lett.* **2005**, *86*, 112510.
[7] F. Giesen, J. Podbielski, B. Botters, D. Grundler, *Phys. Rev. B* **2007**, *75*, 184428.
[8] A. Khitun, K. L. Wang, *Proceedings of the Third International Conference on Information Technology*, New Generations ITNG '06, **2006**, 747.
[9] V. V. Kruglyak, R. J. Hicken, *J. Magn. Magn. Mater.* **2006**, *306*, 191.
[10] S. Choi, K.-S. Lee, K. Y. Guslienko, S.-K. Kim, *Phys. Rev. Lett.* **2007**, *98*, 087205.
[11] V. E. Demidov, S. O. Demokritov, K. Rott, P. Krzysteczko, G. Reiss, *Appl. Phys. Lett.* **2008**, *92*, 232503.
[12] S. A. Nikitov, P. Tailhades, C. S. Tsai, *J. Magn. Magn. Mater.* **2001**, *236*, 320.
[13] M. Krawczyk, H. Puszkarski, *Cryst. Res. Technol.* **2006**, *41*, 547.
[14] J. D. Joannopoulos, S. G. Johnson, J. N. Winn, R. D. Meade, *Photonic Crystals – Molding the Flow of Light*, 2nd Edn, Princeton University Press, Princeton/Oxford, US/UK **2008**.
[15] K. Y. Guslienko, A. N. Slavin, *Phys. Rev. B* **2005**, *72*, 014463.
[16] J. P. Park, P. Eames, D. M. Engebretson, J. Berezovsky, P. A. Crowell, *Phys. Rev. Lett.* **2002**, *89*, 277201.
[17] W. K. Hiebert, A. Stankiewicz, M. R. Freeman, *Phys. Rev. Lett.* **1997**, *79*, 1134.
[18] M. Buess, R. Höllinger, T. Haug, K. Perzlmaier, U. Krey, D. Pescia, M. R. Scheinfein, D. Weiss, C. H. Back, *Phys. Rev. Lett.* **2004**, *93*, 077207.
[19] J. Topp, J. Podbielski, D. Heitmann, D. Grundler, *Phys. Rev. B* **2008**, *78*, 024431.
[20] K. Perzlmaier, G. Woltersdorf, C. H. Back, *Phys. Rev. B* **2008**, *77*, 054425.
[21] D. Grundler, F. Giesen, J. Podbielski, in: *Spin Wave Confinement*, (Ed: S. O. Demokritov), World Scientific, Singapore **2008**, see also the further chapters therein.
[22] M. Bailleul, D. Olligs, C. Fermon, *Phys. Rev. Lett.* **2003**, *91*, 137204.
[23] J. Topp, J. Podbielski, D. Heitmann, D. Grundler, *J. Appl. Phys.* **2009**, *105*, 07D302.

© 2009 WILEY-VCH Verlag GmbH & Co. KGaA, Weinheim

[24] M. Kostylev, P. Schrader, R. L. Stamps, G. Gubbiotti, G. Carlotti, A. O. Adeyeye, S. Goolaup, N. Singh, *Appl. Phys. Lett.* **2008**, *92*, 132504.
[25] A. V. Chumak, A. A. Serga, B. Hillebrands, M. P. Kostylev, *Appl. Phys. Lett.* **2008**, *93*, 022508.
[26] D. Weiss, K. Richter, A. Menschig, R. Bergmann, H. Schweizer, K. von Klitzing, G. Weimann, *Phys. Rev. Lett.* **1993**, *70*, 4118.
[27] R. P. Cowburn, A. O. Adeyeye, J. A. C. Bland, *Appl. Phys. Lett.* **1997**, *70*, 2309.
[28] S. Neusser, B. Botters, D. Grundler, *Phys. Rev. B* **2008**, *78*, 054406.
[29] M. Kostylev, G. Gubbiotti, G. Carlotti, G. Socino, S. Tacchi, C. Wang, N. Singh, A. O. Adeyeye, R. L. Stamps, *J. Appl. Phys.* **2008**, *103*, 07C507.
[30] G. Ctistis, E. Papaioannou, P. Patoka, J. Gutek, P. Fumagalli, M. Giersig, *Nano Lett.* **2009**, *9*, 1.
[31] S. Neusser, B. Botters, M. Becherer, D. Schmitt-Landsiedel, D. Grundler, *Appl. Phys. Lett.* **2008**, *93*, 122501.
[32] J. McCord, L. Schultz, J. Fassbender, *Adv. Mater.* **2008**, *20*, 2090.
[33] M. I. Katsnelson, V. Y. Irkhin, L. Chioncel, A. I. Lichtenstein, R. A. de Groot, *Rev. Mod. Phys.* **2008**, *80*, 315.
[34] K. Baberschke, *Phys. Status Solidi B* **2008**, *245*, 174.
[35] a) Z. L. Xiao, C. Y. Han, U. Welp, H. H. Wang, V. K. Vlasko-Vlasov, W. K. Kwok, D. J. Miller, J. M. Hiller, R. E. Cook, G. A. Willing, G. W. Crabtree, *Appl. Phys. Lett.* **2002**, *81*, 2869; b) S. Martens, O. Albrecht, K. Nielsch, D. Görlitz, *J. Appl. Phys.* **2009**, *105*, 07C113.
[36] P. Chu, D. L. Mills, R. Arias, *Phys. Rev. B* **2006**, *73*, 094405.
[37] R. Qiu, Z. Zhang, L. Guo, C. Ying, J. Liang, *Phys. Status Solidi B* **2006**, *243*, 1983.
[38] L. Giovannini, F. Montoncello, F. Nizzoli, *Phys. Rev. B* **2007**, *75*, 024416.
[39] J.-M. Qiu, J.-P. Wang, *Adv. Mater.* **2007**, *19*, 1703.
[40] O. Kasyutich, A. Sarua, W. Schwarzacher, *J. Phys. D: Appl. Phys.* **2008**, *41*, 134022.
[41] E. V. Shevchenko, M. I. Bodnarchuk, M. V. Kovalenko, D. V. Talapin, R. K. Smith, S. Aloni, W. Heiss, A. P. Alivisatos, *Adv. Mater.* **2008**, *20*, 4323.

WILEY InterScience® DISCOVER SOMETHING GREAT
© 2009 WILEY-VCH Verlag GmbH & Co. KGaA, Weinheim